© 2017. Published by The Company of Biologists Ltd | Development (2017) 144, 1118-1127 doi:10.1242/dev.143966

Development of a human cardiac organoid injury model reveals innate regenerative potential

Holly K. Voges[1], Richard J. Mills[1], David A. Elliott[2], Robert G. Parton[3,4], Enzo R. Porrello[1,*] and James E. Hudson[1,*]

ABSTRACT

The adult human heart possesses a limited regenerative potential following an ischemic event, and undergoes a number of pathological changes in response to injury. Although cardiac regeneration has been documented in zebrafish and neonatal mouse hearts, it is currently unknown whether the immature human heart is capable of undergoing complete regeneration. Combined progress in pluripotent stem cell differentiation and tissue engineering has facilitated the development of human cardiac organoids (hCOs), which resemble fetal heart tissue and can be used to address this important knowledge gap. This study aimed to characterize the regenerative capacity of immature human heart tissue in response to injury. Following cryoinjury with a dry ice probe, hCOs exhibited an endogenous regenerative response with full functional recovery 2 weeks after acute injury. Cardiac functional recovery occurred in the absence of pathological fibrosis or cardiomyocyte hypertrophy. Consistent with regenerative organisms and neonatal human hearts, there was a high basal level of cardiomyocyte proliferation, which may be responsible for the regenerative capacity of the hCOs. This study suggests that immature human heart tissue has an intrinsic capacity to regenerate.

KEY WORDS: Cardiac organoids, Cardiac tissue engineering, Injury model, Regeneration

INTRODUCTION

In contrast to the mammalian heart, lower vertebrates such as axolotls, newts and zebrafish are able to completely regenerate damaged myocardium following cardiac injury in adult life (Porrello and Olson, 2014). These regenerative animals initially deposit extracellular matrix (ECM) proteins, similar to the response of the mammalian heart following injury; but, in contrast, the scar tissue is degraded and replaced by proliferating cardiomyocytes (Chablais et al., 2011; Mercer et al., 2013; Poss et al., 2002). Recently, this regenerative capacity has been shown to exist in a mammalian system. It has been shown that newborn rodent hearts possess an endogenous regenerative capacity following multiple forms of injury, such as ventricular resection (Porrello et al., 2011; Mahmoud et al., 2014), cryoinjury (Jesty et al., 2012; Darehzereshki et al., 2015), coronary artery ligation (Haubner et al., 2012; Porrello et al., 2013; Mahmoud et al., 2014) and genetic cardiomyocyte ablation (Lavine et al., 2014). As observed in regenerating lower vertebrates, the replacement of lost cardiomyocytes in newborn rodents is dependent upon endogenous cardiomyocyte proliferation (Porrello et al., 2011, 2013). This regenerative and proliferative capacity rapidly diminishes during the first 7 days after birth in mice (Porrello et al., 2011), suggesting that the cardiac regenerative capacity is developmentally regulated in mammals. It is currently unknown whether a similar regenerative window exists in the human heart, as there is no viable model system to study this process.

The possibility of cardiac regeneration in human children and infants was first described almost a century ago following the identification of split myocardial fibers in children infected with diphtheria (Macmahon, 1937; Warthin, 1924). These early studies support the concept of a regenerative window during human heart development. Furthermore, recent case studies have emerged documenting complete functional recovery of newborn human hearts following myocardial infarction (MI) (Haubner et al., 2016; Boulton et al., 1991). Haubner and colleagues made the striking observation of complete functional recovery of a newborn human heart following a severe myocardial infarction caused by coronary artery occlusion (Haubner et al., 2016). Remarkably, the child was able to completely recover cardiac function within weeks of the initial ischemic insult, which translated into long-term restoration of cardiac function. However, the authors were unable to determine whether this phenomenon represented a true regenerative process or whether it was due to stunning or to hibernation of the myocardium following reperfusion. Thus, there is an unmet need to develop a human model for assessing the intrinsic regenerative potential of immature human heart tissue.

Recent advances in stem cell biology and tissue engineering have provided unprecedented access to human heart tissue for basic biological studies, disease modeling, drug screening and regenerative medicine applications (Eder et al., 2016; Eschenhagen et al., 2012). Robust protocols have been developed to differentiate human pluripotent stem cells (hPSC), such as embryonic stem cells (ESCs) and induced pluripotent stem cells (iPSCs), to produce cardiomyocytes (Hudson and Zimmermann, 2011). In addition, tissue-engineering approaches have been applied to stem cell-derived cardiomyocytes to enhance their physiological relevance by recapitulating the native 3D environment (Zhang et al., 2013). Enhanced maturation and functionality of hPSC-CM can be achieved by culturing in mechanically loaded engineered heart tissues (Yang et al., 2014). Mechanical loading is used in these cultures as it improves sarcomere length, organization of contractile proteins and functionality (Tulloch et al., 2011; Fink et al., 2000). 3D-engineered human cardiac organoids (hCOs) therefore provide a functional model with which to study human cardiac biology and regenerative phenomena using experimental manipulations that are not feasible

[1]School of Biomedical Sciences, The University of Queensland, St Lucia, Queensland 4072, Australia. [2]Murdoch Children's Research Institute, Royal Children's Hospital, School of Biosciences, The University of Melbourne, Parkville, Victoria 3052, Australia. [3]Institute for Molecular Bioscience, The University of Queensland, St Lucia, Queensland 4072, Australia. [4]Centre for Microscopy and Microanalysis, The University of Queensland, St Lucia, Queensland 4072, Australia.

*Authors for correspondence (e.porrello@uq.edu.au, j.hudson@uq.edu.au)

J.E.H., 0000-0003-0832-9356

Received 22 August 2016; Accepted 17 January 2017

Development (2017) 144, 1118-1127 doi:10.1242/dev.143966

in vivo. This study for the first time characterizes the injury response of hCOs following cryoinjury *in vitro*. We report that hCOs resemble fetal/neonatal-like human cardiac tissue and undergo functional recovery, in the absence of fibrosis or hypertrophy, following injury. These findings suggest that regenerative capacity is an intrinsic property of immature human heart tissue.

RESULTS

hCOs possess features of immature human myocardium

Flow cytometry was used to characterize the major cell types derived from a protocol based on a previously described 2D cardiac differentiation protocol (Fig. 1A) (Hudson et al., 2012). At day 15 of differentiation, cultures were stained with markers (for validation, see Fig. S1) for cardiomyocytes (α-actinin and cardiac troponin T), stromal cells (CD90), endothelial cells (CD31) and leukocytes (CD45 and CD14), which are the major cell types present in the myocardium *in vivo* (Pinto et al., 2016; Bergmann et al., 2009; Zhou and Pu, 2016). Flow analysis revealed that the majority of the total cell population was positive for cardiomyocyte markers, with ∼60-70% of cells expressing cTnT or α-actinin (Fig. 1B). The majority of the non-myocyte population comprised $CD90^+$ stromal cells, with 14 ±3% $CD90^+$ cells present at day 15 of differentiation in the HES3 ESC line and a slightly higher proportion of $CD90^+$ cells (35±3%) present in the H9 ESC line (Fig. 1B). These ratios of cardiomyocytes to $CD90^+$ stromal cells are comparable with those seen in the embryonic or neonatal rodent heart (Ieda et al., 2009). Fewer than 1% of cells were positive for CD45/CD14 and CD31 markers in both cell lines, indicating that leukocytes and endothelial cells are largely absent from this *in vitro* culture system.

To highlight the relative immaturity of hESC-derived cells compared with adult cardiac cells, gene expression profiling of key sarcomeric proteins, which change during cardiac maturation, were analyzed and compared with native adult human whole heart (Fig. 1C). β-Myosin heavy chain (*β-MHC*, also known as *MYH7*), myosin light chain 2v (*MLC2v* also known as *MYL2*) and the N2B isoform of titin (*TTN N2B*) (Opitz et al., 2004) are the dominant isoforms expressed in adult cardiomyocytes. By contrast, alpha-myosin heavy chain (*α-MHC* also known as *MYH6*), myosin light chain 2a (*MLC2a* also known as *MYL7*, and the N2BA isoform of titin (*TTN N2BA*) are the dominant isoforms expressed during early embryonic development and in standard 2D cultures of hPSC-derived cardiomyocytes (Veerman et al., 2015). qPCR analysis revealed that hCOs had much lower expression of the adult sarcomeric isoforms (*β-MHC*, *MLC2v* and *TTN N2B*) and higher expression of the fetal sarcomeric isoforms (*MLC2a*), compared with native adult human heart tissue (Fig. 1C). These findings indicate that hCOs display an immature phenotype, as previously described for hPSC-derived cardiomyocytes (Synnergren et al., 2012).

Using differentiated cardiac cells derived from H9, HES3 and HES3 NKX2-$5^{eGFP/w}$ cell lines, hCOs were formed using previously described bioengineering approaches (Zimmermann et al., 2002; Tiburcy et al., 2014; Soong et al., 2012). Briefly, cardiac cells were cast in circular wells (Fig. 1D) in collagen 1. After 5 days in culture, the 3D circular tissues were placed around elastic posts to impose mechanical loading on the tissues to promote cardiomyocyte alignment and functionality (Fig. 1D). Immunohistochemistry was used to characterize the morphology and distribution of cells present in hCOs. Sarcomeric proteins, such as α-actinin, tropomyosin and titin (Fig. 1E), showed cardiomyocyte striation throughout the hCOs, which also expressed the cardiac-specific marker myosin light chain 2v (MLC2v) (Fig. 1E). Stromal cells surrounded cardiomyocytes throughout hCOs, which are vital for maintaining tissue architecture (Fig. 1E and data not shown). The endothelial marker CD31 was not detected in our hCO constructs (Fig. 1E). Transmission electron microscopy (TEM) of sectioned hCOs revealed fully formed Z-discs, which, in combination with α-actinin staining, is indicative of highly organized sarcomeres (Fig. 1E). Cardiomyocyte coupling was evident in 3D tissues; however, β-catenin and pan-cadherin localization was circumferential rather than polarized to the cardiomyocyte ends, which is indicative of structurally immature cardiomyocytes rather than an adult phenotype (Fig. 1E).

We next assessed the functionality of hCOs by analyzing contractile force in response to changes in extracellular calcium. Organ bath recordings showed that hCO increased their force of contraction in response to increasing concentrations of extracellular calcium (Fig. 1F). Increasing calcium concentration had a positive inotropic effect in HES3 hCOs (Fig. 1F), which is a characteristic physiological property of cardiac muscle.

Together, these data characterize the cellular composition, protein and gene expression of the hCO constructs. This characterization indicates that hCO constructs contain primarily cardiomyocytes and stromal cells at a ratio that is comparable with the fetal/neonatal heart, and form functional sarcomere units that display physiological inotropic responses to calcium. Overall, the hCOs resemble immature myocardium and provide a physiologically relevant *in vitro* model of fetal/neonatal human heart muscle.

Cryoinjury induces cell death and tissue ablation in hCOs

In order to determine whether immature hCOs can regenerate following injury, we established a cryoinjury model. The cryoinjury model was chosen over hypoxia-reoxygenation models so that we could cause cardiomyocyte death in a localized area while maintaining viable tissue remote to the injury zone. This more closely recapitulates cardiac injury in cases where myocardial infarction causes death to a particular region of the heart. Cryoinjury models have been used extensively in the literature to study cardiac regeneration in lower vertebrates and neonatal rodents, as the technique results in localized cell death with viable surrounding tissue (Chablais and Jazwinska, 2012; Robey and Murry, 2008; Ciulla et al., 2004; Darehzereshki et al., 2015). Cryoinjury was induced in hCOs by application of a small dry-ice probe that covered the width and one-third of the length of the hCO (∼100 µm×250 µm). Application of a dry-ice probe was the preferred method of cryoinjury compared with using a metallic cryoprobe, as when we attempted to use a metallic probe it became stuck to the tissue.

We next evaluated the extent of tissue damage caused by our cryoinjury protocol. Using a cardiomyocyte-specific green fluorescent protein (GFP) cell line, HES3 NKX2-$5^{eGFP/w}$, hCOs were visualized in real time (Fig. 2Aii, iii). Cryoinjury resulted in an isolated loss of GFP expression in ∼15% of hCOs (Fig. 2Aiii), which did not compromise overall tissue integrity (Fig. 2Ai). Localized cryoinjury was also confirmed with immunohistochemistry, which revealed the same pattern of localized loss of α-actinin and nuclear staining in HES3 hCOs, which was absent in controls (Fig. 2B,C). Cryoinjury was further validated using two independent cell death assays for lactate dehydrogenase (LDH) and cardiac troponin I (cTnI) release, which are both used clinically to detect suspected myocardial damage (Thygesen et al., 2012; Skillen, 1984). Cryoinjury in HES3 and HES3 NKX2-$5^{eGFP/w}$ hCOs resulted in an approximately threefold increase in LDH release into the media compared with uninjured controls (Fig. 2D). cTnI levels were also evaluated as a cardiomyocyte-specific readout of cell death 4 h following cryoinjury. Similarly, cryoinjury caused an approximately threefold increase in cTnI levels in HES3 and HES3 NKX2-$5^{eGFP/w}$ hCOs (Fig. 2E). These findings confirm that cryoinjury of hCO induces localized cardiomyocyte death.

Development (2017) 144, 1118-1127 doi:10.1242/dev.143966

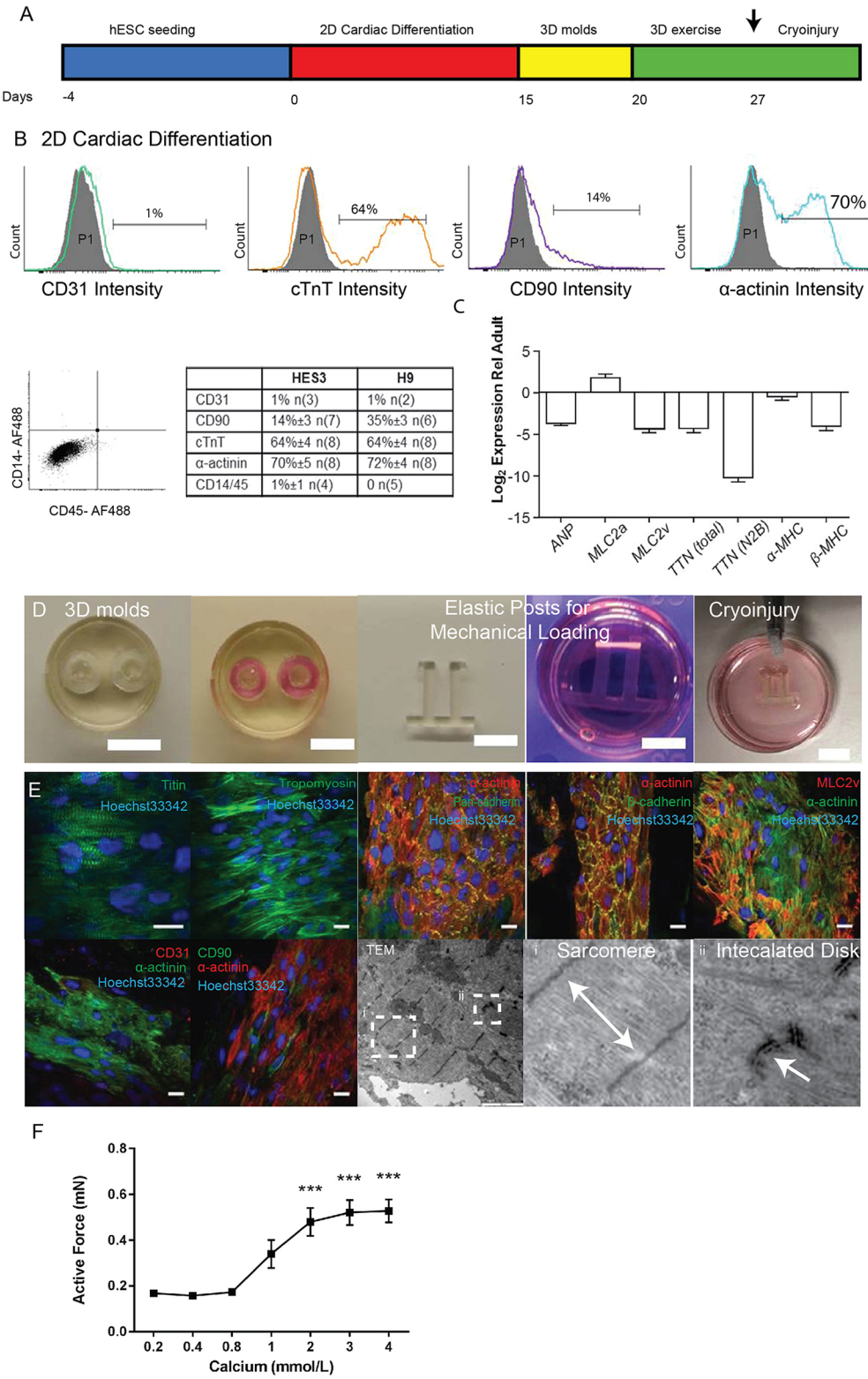

Fig. 1. hCOs display properties of immature human heart tissue. (A) Timeline of the differentiation protocol and hCO formation. (B) Representative flow cytometry analysis of the cell types present after the cardiac differentiation protocol (day 15). The average percentage of cell types after differentiation of H9 and HES3 embryonic stem cells is shown. (C) Gene expression analysis of key cardiac markers compared with adult human heart. (D) Representative image of the PDMS molds and PDMS poles for mechanical loading used to form the hCOs. hCOs in culture medium on exercisers and with dry-ice probe. Scale bars: 1 mm. (E) High-magnification confocal images of hCOs, outlining cell-cell junctions (pan cadherin and β-catenin) and sarcomeric proteins (titin and tropomyosin). High-magnification confocal images of hCOs stained with cardiac (MLC2v), stromal cell (CD90) and endothelial cell markers (CD31). Scale bars: 20 µm. High-magnification transmission electron microscopy (TEM) image of sectioned hCOs. Scale bar: 0.5 µm. (i) Two Z-discs; double-headed arrow indicates length of sarcomere. (ii) Cell-cell junction (arrow). (F) Effect of increasing calcium concentration on HES3 hCO force of contraction using an organ bath (n=3), ***P<0.001 versus 0.2 mM Ca^{2+} analyzed using ANOVA with Sidak's multiple comparison post-test.

Lack of fibrotic or hypertrophic responses following cryoinjury in hCOs

Fibrosis and hypertrophy are characteristic hallmarks of the adult reparative response following MI in humans. Similarly, adult mammals deploy a fibrotic and hypertrophic response following cryoinjury (Yang et al., 2010, 2011). By contrast, the neonatal heart is characterized by an absence of fibrosis and hypertrophy following cardiac injury (Porrello et al., 2011, 2013). In order to determine whether hCOs displayed adult- or neonatal-like responses to cardiac injury, we quantified markers of fibrosis and hypertrophy in HES3 and HES3 NKX2-5$^{eGFP/w}$ hCOs following cryoinjury. Trichrome staining was initially performed to visualize the deposition of ECM proteins. However, this analysis was confounded by the collagen 1 matrix that was used to make hCO. We therefore analyzed ECM gene expression

Development (2017) 144, 1118-1127 doi:10.1242/dev.143966

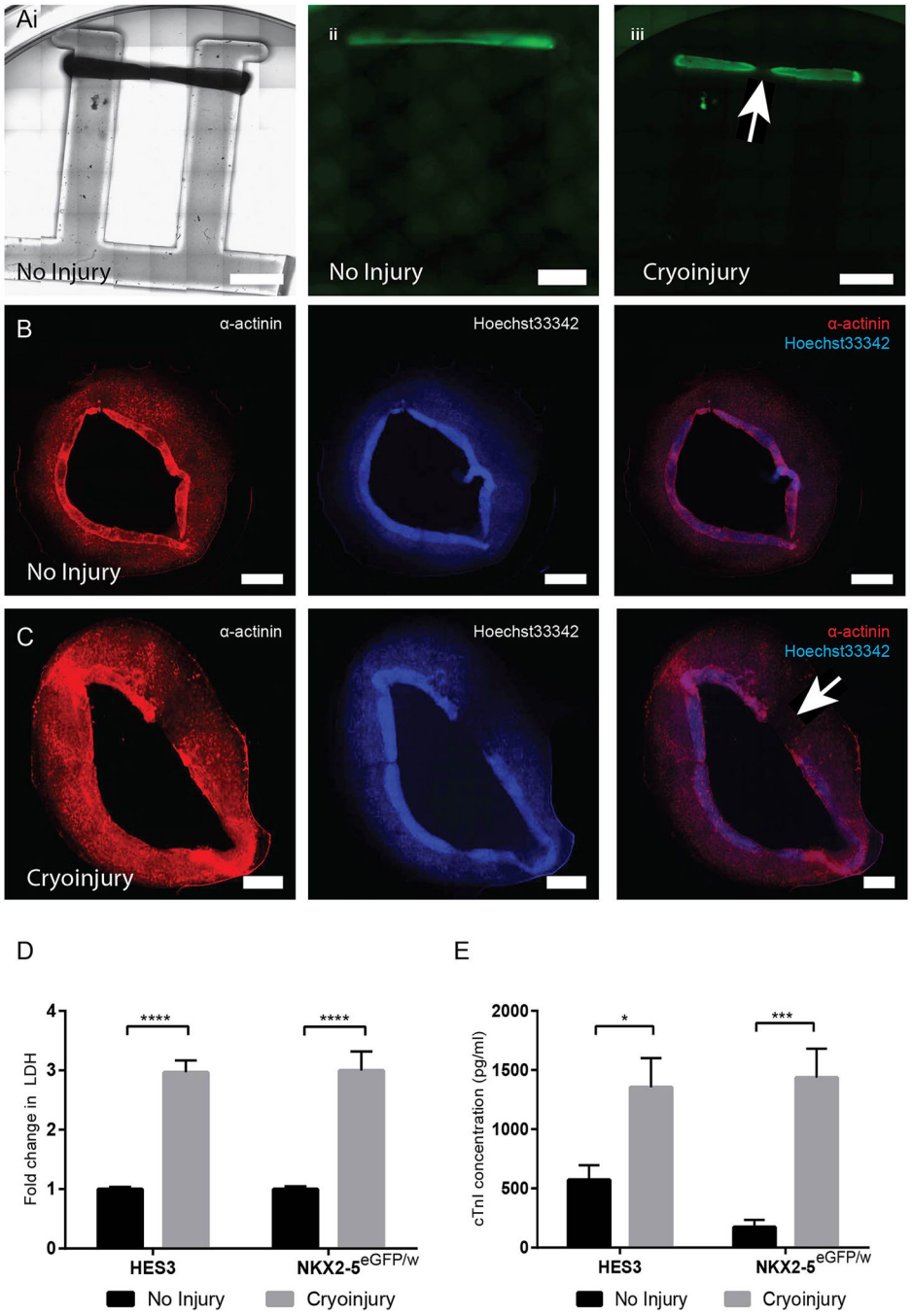

Fig. 2. Cryoinjury of hCOs results in localized cell death and reduced contractile function. (Ai) Live HES3 NKX2-5$^{eGFP/w}$ hCOs on exercise poles in culture. (ii) GFP imaging of cardiomyocytes in live uninjured control hCOs. (iii) GFP imaging of cardiomyocytes in cryoinjured hCOs; arrow indicates loss of cardiomyocytes. Scale bars: 2 mm. (B) Whole-mount immunofluorescent image of an uninjured hCO stained with α-actinin and Hoechst33342. (C) Whole-mount immunofluorescent image of a cryoinjured hCO 3 days post-cryoinjury; arrow indicates site of injury. Scale bars: 1 mm. (D) Lactate dehydrogenase change in HES3 (n=33, over 9 experiments) and HES3 NKX2-5$^{eGFP/w}$ (n=18, over 6 experiments) hCOs in response to cryoinjury. ****P<0.0001, using Student's t-test. (E) Cardiac troponin I detected in HES3 and HES3 NKX2-5$^{eGFP/w}$ hCO medium 4 h post-cryoinjury (n=5, 3 experiments). *P<0.02; ***P<0.001, using Student's t-test.

at 1, 3, 7, 10 and 14 days post-cryoinjury, as this time frame has been characterized in other *in vivo* cryoinjury models (Gonzalez-Rosa et al., 2011; Sun et al., 2000). In contrast to the adult response to cardiac injury *in vivo*, cryoinjury did not cause a global upregulation of ECM genes or integrins, including collagen type 1 (*COL1A1*), collagen type 3 (*COL3A1*), elastin (*ELN*), fibronectin (*FN1*), integrin alpha 1 (*ITGA1*) and laminin γ subunits (*LAMC1*) (Fig. S2A). At 14 days post-cryoinjury, *FN1*, *ELN* and *IGTA1* were upregulated. Therefore we used an alternative method to confirm whether there was fibrosis and analyzed protein expression with western blot analysis at the same time point. Quantification of fibronectin protein expression revealed that there was no increase following cryoinjury (Fig. S2B). These results indicate that cryoinjury does not cause a collagenous fibrotic response in immature hCOs.

To characterize hypertrophy in this model, we analyzed the expression of several cardiac stress genes, including atrial natriuretic peptide (*ANP* also known as *NPPA*) and skeletal actin (*ACTA1*). qPCR analysis revealed that there was no significant upregulation of *ANP* at 1, 3, 7, 10 or 14 days post-cryoinjury or of *ACTA1* at 1, 3, 7 and 10 days post-cryoinjury (Fig. S2C). There was an upregulation of *ACTA1* at 14 days post-cryoinjury, whereas ANP was highly variable in both uninjured and cryoinjury groups. To formally assess hypertrophy, histological analysis of cardiomyocyte cell size was performed to quantify the cross-sectional area of cardiomyocytes at 14 days post-injury (Fig. S2Di). This robust analysis revealed that cryoinjury did not cause an increase in cell size in HES3 NKX2-5$^{eGFP/w}$ hCOs at day 14 post-injury (Fig. S2Dii). Collectively, these data indicate that cryoinjury does not induce hypertrophy in immature hCOs.

Development (2017) 144, 1118-1127 doi:10.1242/dev.143966

hCOs have high basal rates of cardiomyocyte proliferation before and after cryoinjury

In contrast to adults, neonatal rodents are able to regenerate following cardiac injury, including non-transmural cryoinjury (Darehzereshki et al., 2015). Cardiac regeneration in neonates is associated with high basal rates of cardiomyocyte proliferation, which increases further upon injury in some models (Porrello et al., 2013; Bryant et al., 2014). As hCOs did not undergo fibrosis or hypertrophy following cryoinjury, we examined whether cardiomyocyte cell cycle activity was upregulated. Cardiomyocyte cell cycle activity was quantified by immunohistochemical analysis of Ki-67+ (Fig. 3A,B) and phosphorylated Histone H3 ($pH3^+$) (Fig. 3D,E) cardiomyocytes at 3 days post-cryoinjury. A trend towards increased numbers of $Ki\text{-}67^+$ cardiomyocytes (Fig. 3C) and a significant increase in $pH3^+$ cardiomyocytes with disassembled sarcomeres (Fig. 3F) were detected in HES3-derived hCOs following cryoinjury. However, cryoinjury did not cause a significant increase in $pH3^+$ cardiomyocytes in H9 or HES3 NKX2-$5^{eGFP/w}$ hCO (Fig. 3F), suggesting that this proliferative response varies between cell lines. Nevertheless, even in the absence of injury, cardiomyocyte proliferation rates in hCO constructs were similar to neonatal human heart tissue (Polizzotti et al., 2015), providing further support for the notion that this model recapitulates immature human myocardium. To confirm repopulation of the hCOs with cardiomyocytes, we tracked GFP intensity of hCOs fabricated using the cardiomyocyte-specific reporter line HES3 NKX2-$5^{eGFP/w}$.

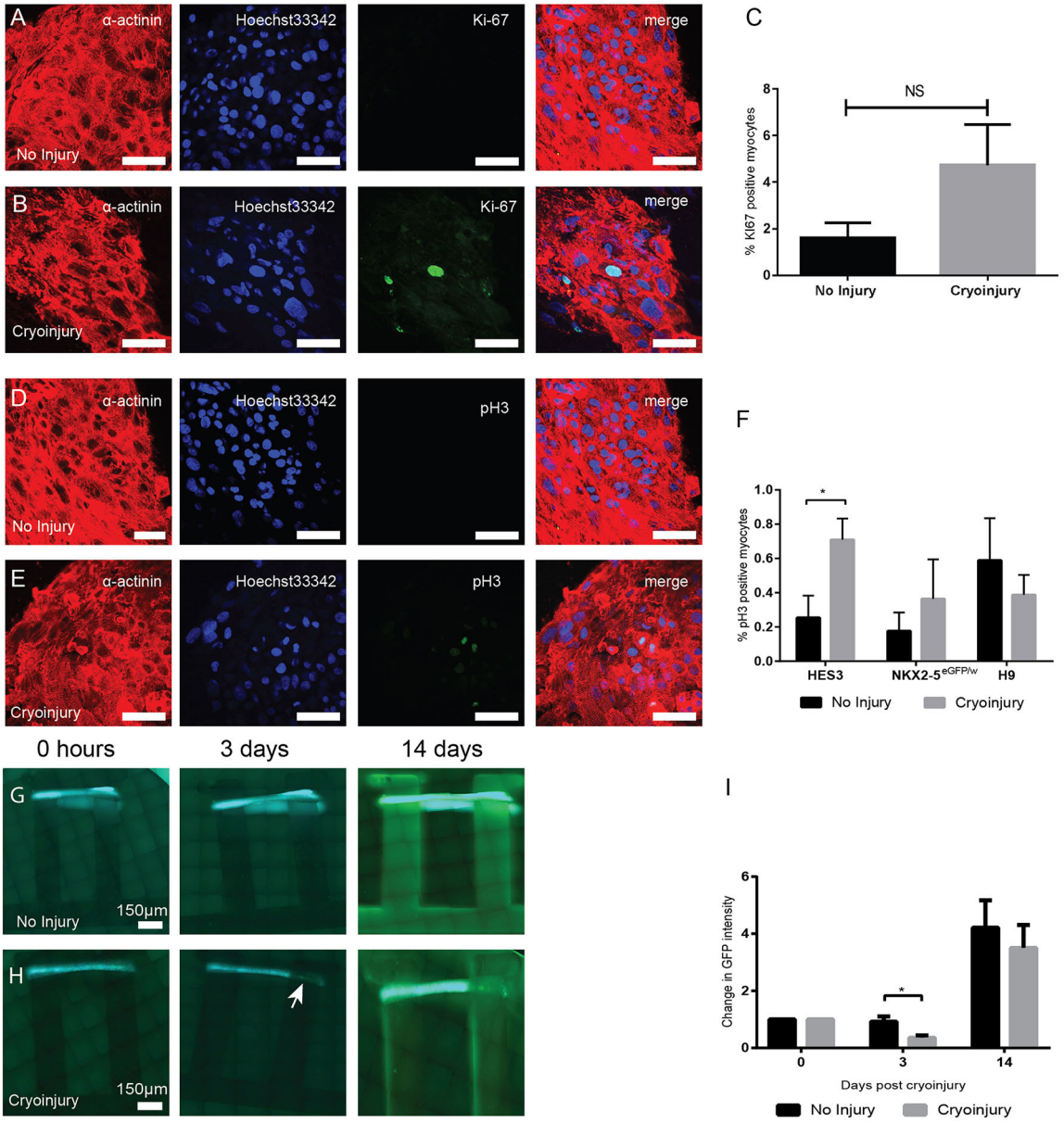

Fig. 3. Cryoinjury is associated with high basal rates of cardiomyocyte proliferation in hCOs. (A,B) High-magnification images of (A) control HES3 hCOs and (B) cryoinjured HES3 hCOs stained with α-actinin, Ki-67 and Hoechst33342. (C) Quantification of Ki-67-positive cardiomyocytes in HES3 hCOs (n=12, four experiments). (D,E) High-magnification images of (D) control HES3 hCOs and (E) cryoinjured HES3 hCOs stained with α-actinin, pH3 and Hoechst33342. (F) Quantification of pH3-positive cardiomyocytes in HES3 hCOs (n=5-7), H9 HCOs (n=7-10) and HES3 NKX2-$5^{eGFP/w}$ hCOs (n=5 or 6). *P<0.05, using Student's t-test. Scale bars: 50 μm. (G,H) GFP images created using HES3 NKX2-$5^{eGFP/w}$-derived hCOs showing (G) uninjured hCOs and (H) cryoinjured hCOs at 0, 3 and 14 days post-cryoinjury live in culture. (I) GFP (cardiomyocyte) intensity at 0, 3 and 14 days post-cryoinjury (n=4). *P<0.05, using Student's t-test.

Development (2017) 144, 1118-1127 doi:10.1242/dev.143966

Consistent with cardiomyocyte death, we found that GFP intensity was reduced 3 days post-cryoinjury (Fig. 3G,H). Inspection of HES3 NKX2-5$^{eGFP/w}$ tissues at day 14 indicated that the majority of the injured region had regenerated and GFP intensity levels were indistinguishable from control uninjured hCOs after 14 days (Fig. 3I).

hCOs regenerate and recover cardiac function following cryoinjury

Owing to their immature physiological properties, high rates of cardiomyocyte proliferation and lack of a fibrotic or hypertrophic response to cryoinjury, we next tested whether hCOs regenerated following cryoinjury. Contractile force was determined at multiple time points (Fig. 4A) following cryoinjury using electrical pacing at 1 Hz with video analysis and a customized motion tracking computer program (see Materials and Methods and Fig. S3). At 6 h following cryoinjury, there was a 53% and a 57% reduction in active force in HES3 and HES3 NKX2-5$^{eGFP/w}$ hCOs, respectively (Fig. 4B). Similarly, a trend towards active force reduction (65%, P=0.07) was observed 6 h after cryoinjury in H9 hCOs but this failed to reach statistical significance (Fig. 4B). Remarkably, active force recovered 14 days post-cryoinjury, measured using electrical pacing at 1 Hz with video analysis and a customized motion tracking computer program (Fig. 4C). We also used organ bath experiments to measure active force at 14 days post-cryoinjury. This analysis indicated that contractile forces had substantially recovered in all three hCO lines towards hCO forces in the uninjured tissues (Fig. 4C). These data suggest that immature hCOs are able to functionally recover following cryoinjury.

Macrophages have been implicated in neonatal heart regeneration where monocyte depletion impaired angiogenesis and abolished the regenerative response to infarction (Aurora et al., 2014). Importantly, neonatal monocyte depletion impaired angiogenesis but did not affect cardiomyocyte proliferation *in vivo*. As our hCOs do not require vascularization and endothelial cells are absent from the hCOs, we tested whether the addition of monocytes from cord blood or adult humans would impact fibrosis and cardiomyocyte proliferation in hCOs. We validated monocyte survival at 3 days post-cryoinjury with immunohistochemical staining and gene expression analysis of the monocyte marker CD14 (Fig. S4A,B). There was no significant change in Ki-67-positive cardiomyocytes following cryoinjury with cord blood or adult CD14+ monocyte co-culture (Fig. S4C). We also assessed gene expression of extracellular matrix genes *COL1A1*, *COL3A1*, *ELN*, *FN1*, *ITGA1* and *LAMC1* at 3 days post-cryoinjury with co-culture of both cord blood and adult human CD14+ monocytes (Fig. S4D). We found that there was no significant upregulation of extracellular matrix genes following cryoinjury at this time point with co-culture of either monocyte population. Consistent with *in vivo* data, these results indicate that monocytes do not regulate the proliferative response of immature hCOs.

We next tested whether the recovery of the hCO functionality after cryoinjury was due to cardiomyocyte proliferation. To test this hypothesis, we inhibited cardiomyocyte proliferation with the chemotherapeutic agent mitomycin C (Fig. 4E). Mitomycin C has been shown to inhibit proliferation in a number of cell types *in vitro* while the cells remain viable (Chen et al., 2013; Nieto et al., 2007). We found no cardiomyocyte proliferation marked by pH3-positive cardiomyocytes treatment with mitomycin C 6 h after cryoinjury (n=3 hCOs, 1893 cells counted, Fig. 4F). We found that there was no effect on force of contraction after 14 days with no injury indicating that hCO viability and functionality was not effected by mitomycin C treatment (Fig. 4G). However, mitomycin C prevented functional recovery of force of contraction analyzed 14 days after cryoinjury (Fig. 4G). This indicates that functional recovery following cryoinjury requires proliferation.

DISCUSSION

A major limitation to studying human cardiac regeneration is the lack of models and tissue samples to study the repair responses of the human heart following injury. To date, a human model of acute cardiac injury has not been achieved. Instead, most research into regeneration following cardiac injury has relied on the use of animal models. hCOs have been proposed as a physiologically relevant model of the human heart (Caspi et al., 2007; Schaaf et al., 2011; Tiburcy et al., 2011), which has a variety of applications from drug screening to studying human cardiac biology. However, hCOs have yet to be applied to meet the demand for an *in vitro* system to study cardiac regenerative phenomena. To address this problem and provide insight into the endogenous repair processes of the immature human heart, we developed and characterized a human *in vitro* model of acute cryoinjury. Importantly, our hCO constructs were found to be physiologically representative of the native immature human heart. This finding is consistent with the characterization of other hCO constructs, which were also found to be most comparable with the fetal human heart (Veerman et al., 2015). Remarkably, hCOs were able to completely recover cardiac function following cryoinjury, displaying many of the hallmarks of regenerative neonatal heart tissue.

The major finding from this study is that immature human heart tissue possesses an innate ability to regenerate following injury. Interestingly, in our *in vitro* system, myocytes possess an endogenous ability to recover contractile force following injury, which occurs independently of other infiltrating/resident cell types that are present within the *in vivo* setting. As the immune system has been heavily associated with reparative responses following cardiac injury in many animal systems (Nahrendorf et al., 2007; Evans et al., 2013; Frantz and Nahrendorf, 2014; Aurora et al., 2014), an interesting implication of our finding is that immune cells are not required for functional recovery of immature heart tissue. Furthermore, the addition of monocytes in our studies did not have any impact on cardiomyocyte proliferation, which is consistent with *in vivo* observations (Aurora et al., 2014). This suggests that immature human heart muscle may possess an intrinsic ability to mount a regenerative response, which occurs even in the absence of inflammation and angiogenesis. However, it should be noted that our *in vitro* model does not fully recapitulate the *in vivo* setting, which could be important for studying the actions of the immune system of the regenerative process. As macrophages predominantly influence the angiogenic response to infarction in neonates (Aurora et al., 2014), co-culture of hCOs with endothelial cells and immune cells could provide another important avenue for future investigation.

In regenerating animals, damaged myocardium gets replaced by proliferating cardiomyocytes (Poss et al., 2002; Porrello et al., 2011). In our model, we found that cryoinjury only caused a significant increase in myocyte proliferation in one out of three human embryonic stem cell lines. However, hCOs from all three cell lines, HES3, H9 and HES3 NKX2-5$^{eGFP/w}$ exhibited high levels of cardiomyocyte proliferation under basal conditions. Interestingly, the basal levels of proliferation in hCOs were higher than those reported in regenerating zebrafish hearts (Sallin et al., 2015), regenerating neonatal mouse hearts (Porrello et al., 2013) and neonatal human hearts (Polizzotti et al., 2015). In these animals, damaged myocardium is replaced within several weeks, which is comparable with the timeframe over which we detected force

Development (2017) 144, 1118-1127 doi:10.1242/dev.143966

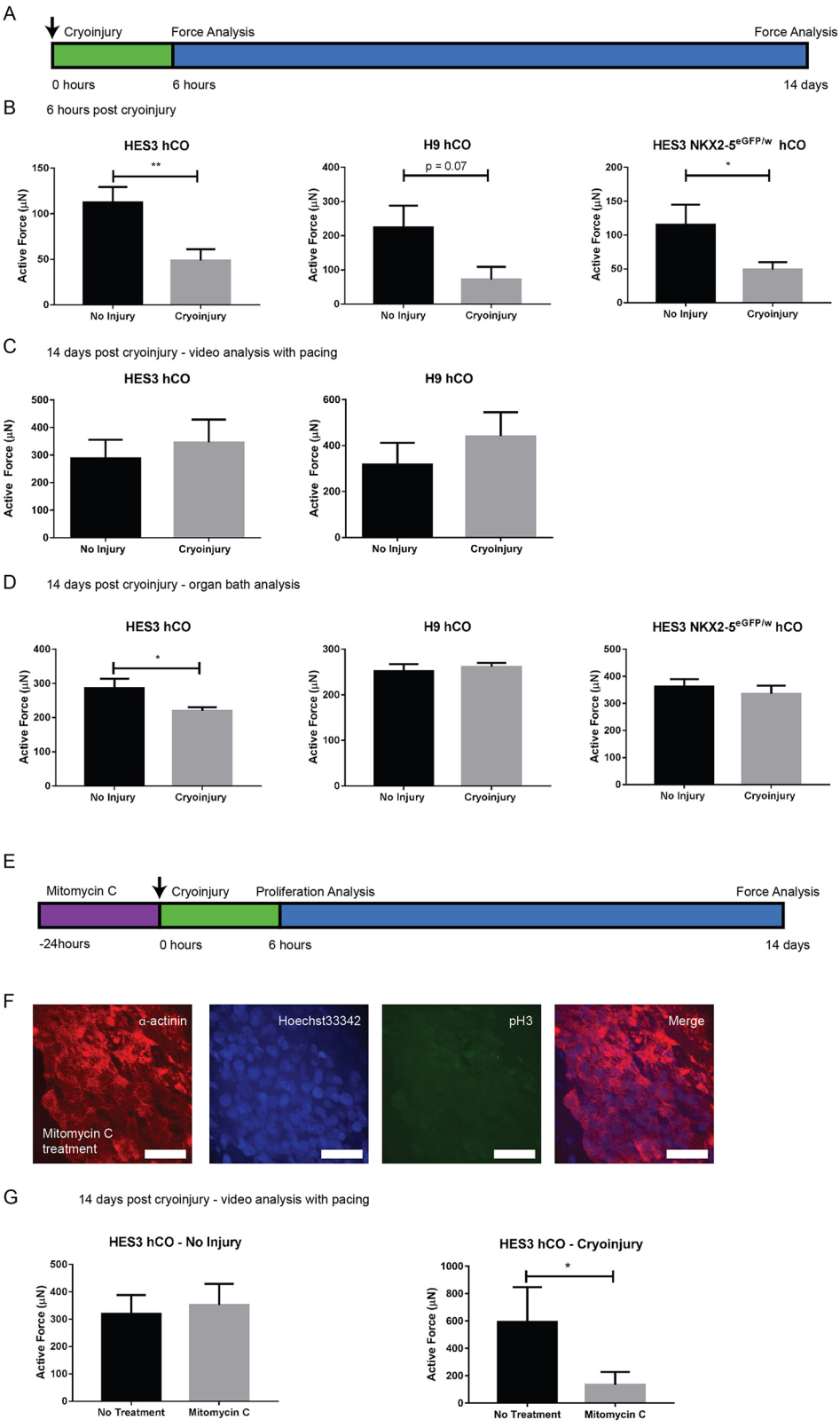

Fig. 4. Functional recovery following cryoinjury of hCOs. (A) Timeline of force analysis following cryoinjury. (B) Change in active force analyzed using tracking of elastic posts and pacing at 1 Hz 6 h post-cryoinjury in HES3 (n=14, three experiments), H9 (n=5) and HES3 NKX2-5$^{eGFP/w}$ (n=4-6) hCOs. **P<0.005 and *P<0.05, using Student's t-test. (C) Change in active force analyzed using tracking of elastic posts and pacing at 1 Hz 14 days post-cryoinjury in HES3 (n=5-6) and H9 (n=5) hCOs. (D) Active force of HES3 (n=14-16, at least four experiments), H9 (n=3 or 4) and HES3 NKX2-5$^{eGFP/w}$ (n=4 or 5) hCOs 14 days post-cryoinjury measured using organ baths. *P<0.05, using Student's t-test. (E) Timeline of mitomycin C treatment protocol. (F) High-magnification image of mitomycin C-treated HES3 hCOs stained with α-actinin, pH3 and Hoechst33342. (G) Analysis of active force generation using tracking of elastic posts and pacing at 1 Hz 14 days post-cryoinjury in HES3 hCOs. Active force comparison of non-injured hCOs [either non-treated (data taken from C) and mitomycin C treated (n=3-6)]. Active force comparison of cryoinjured hCOs [either non-treated or Mitomycin C treated (n=6 or 7)]. *P<0.05, using Mann–Whitney test.

recovery. Our results with mitomycin C inhibition of the cell cycle also indicate that proliferation was responsible for force recovery in our cryoinjury model. In future, it will also be interesting to determine whether more mature cell cycle arrested hCOs display regenerative capacity or not, although this first requires knowledge of the key processes that drive maturation (Yang et al., 2014).

In conclusion, this is the first study to characterize an injury model in hCOs, which we propose to model human fetal hearts. We demonstrate that immature hCO can functionally recover following localized injury. Our study provides novel insight into the endogenous regenerative capacity of the immature human heart, which cannot be investigated in the *in vivo* setting. Our model is

Development (2017) 144, 1118-1127 doi:10.1242/dev.143966

consistent with aspects of neonatal heart regeneration observed *in vivo*: lack of fibrosis, lack of hypertrophy, high baseline proliferation rates, and functional recovery after injury (Porrello et al., 2011, 2013). Our model therefore provides a unique opportunity to interrogate the molecular and cellular mechanisms governing regeneration of immature human heart tissue.

MATERIALS AND METHODS

Human embryonic stem cell culture

Ethical approval for the use of human embryonic stem cells was obtained from The University of Queensland's Medical Research Ethics Committee (2014000801), and was carried out in accordance with the National Health and Medical Research Council of Australia (NHMRC) regulations. All experimental protocols were approved by The University of Queensland's Medical Research Ethics Committee. The hESC lines HES3 and H9 were obtained from WiCell, where informed consent was obtained from all subjects. Additionally, we used the previously published HES3 NKX2-5$^{eGFP/w}$ cardiac reporter line (Elliott et al., 2011). Human ESCs were cultured on Matrigel (Corning)-coated flasks with mTeSR (Stem Cell Technologies) supplemented with 0.5% penicillin-streptomycin (Thermo Fisher Scientific). Cells were seeded at 20,000 cells/cm^2 (HES3 and H9 lines) and 10,000 cells/cm^2 (HES3 NKX2-5$^{eGFP/w}$), passaging with TrypLE (Thermo Fisher) every 3 or 4 days.

Cardiac differentiation protocol

Cardiomyocyte and stromal cell differentiation was achieved using modification of previously described protocols (Hudson et al., 2012), which are further described in the supplementary Materials and Methods. At day 15 of differentiation, cells were harvested with 0.2% collagenase type I (Sigma-Aldrich) in 20% FBS in PBS (with Ca^{2+} and Mg^{2+}) for 60 min, followed by further digestion with 0.25% Trypsin-EDTA (Thermo Fisher Scientific) for 10 min. Trypsin was neutralized with α-MEM medium 10% FBS (supplemented with 1% penicillin-streptomycin, 200 mM L-ascorbic acid) and strained through a 100µm filter. The cells were then resuspended at 4.6×10^6 cells/ml in α-MEM medium for hCO formation.

Forming hCO constructs

hCO constructs were made using differentiated cardiac cells, cold 7.3 mg/ml acid-solubilized bovine collagen 1 (Devro), 0.1 mol l^{-1} sodium hydroxide in milliQ water and 10× Dulbecco's Modified Eagle's medium (DMEM) (Thermo Fisher Scientific) at the ratios outlined in Table S1. Each circular hCO mold (Sylgard 184, Dow Corning) was filled with 140 µl of cell mixture and incubated at 37°C with 5% CO_2 for 30 min to gel before α-MEM medium 10% FBS was added. After 5 days in the mold, hCOs were carefully removed and placed around silicon exercisers using sterile forceps. α-MEM 10% FBS medium was replaced every 2 or 3 days and cryoinjury was performed after 7 days of culture on the exercisers (total differentiation culture of 27 days).

Flow cytometry

On day 15 of cardiac differentiation, cells were harvested as described above. Differentiated cells were stained as described in the supplementary Materials and Methods with the following primary antibodies: α-actinin (Sigma-Aldrich, A7811, 1:1000), cardiac troponin T (Thermo Scientific, MS295P1, 1:400), CD90 (Thermo Fisher Scientific, MAB2067, 1:125), CD31 (eBioscience, 17-0319-42, 1:200), CD14 (Miltenyi Biotech, 130-091-243, 1:1) and CD45 (Miltenyi Biotech, 130-098-043, 1:10). These primary antibodies were validated as shown in Fig. S1.

Cryoinjury protocol for hCOs

On day 27, cryoinjury was performed using a sterile piece of dry ice. Prior to cryoinjury, culture medium was removed to allow precise contact between the topmost arm of the hCOs and the dry ice for 3 s. Medium was then replaced immediately following cryoinjury and incubated at 37°C in 5% CO_2.

Lactate dehydrogenase assay and cardiac troponin I Elisa

Media samples were collected at 4 h post-cryoinjury. Cardiac Troponin I Elisa kit (RayBio) and Lactate dehydrogenase (LDH) Assay (Pierce) were used according to the manufacturer's instructions. For LDH analysis, hCOs were incubated in phenol-free medium (Table S2) following cryoinjury until sample collection when they were returned to α-MEM 10% FBS medium.

Immunohistochemistry

hCO constructs were fixed with 1% paraformaldehyde (PFA) in PBS for 1 h and stained at 4°C with shaking overnight with the following primary antibodies: α-actinin (Sigma, A7811, 1:1000), Ki67 (Cell Signaling Technologies, 9129S, 1:400), pH3 (Merck Millipore, 05-806, 1:200), Pan-cadherin (Sigma, C3678, 1:200), beta-catenin (Cell Signaling Technologies, 8480S, 1:200), Titin (Developmental Studies Hybridoma Bank, 9D10, 5 µg/ml), MLC2V (Protein Tech Group, 10906-1-AP, 1:200) and tropomyosin (Developmental Studies Hybridoma Bank, LC1, 5 µg/ml). hCOs were incubated at 4°C with shaking overnight with the following secondary antibodies: Alexa-fluor goat anti-rabbit 488 (Life Technologies, A11034, 1:400), Alexa-fluor goat anti-mouse 555 (Life Technologies, A21422, 1:400), Hoechst 33342 (Thermo Fisher Scientific, H3570, 1:1000). Images were obtained using Olympus FV1000 Inverted Confocal microscope or Zeiss PALM Microbeam Laser System. For Ki67 and pH3 cardiomyocyte proliferation quantification, multiple images were taken at random locations throughout the tissue and cardiomyocyte proliferation quantification was performed blinded.

Histology

At 14 days post-cryoinjury, hCO constructs were fixed in 1% PFA in PBS for 1 h before histological tissue processing. Transverse sections (6 µm) were cut along the tissue long axis to obtain cardiomyocyte cross-sections before staining with Wheat Germ Agglutinin (50 µg ml^{-1}, Thermo Fisher Scientific) and Hoechst33342 (1:1000). Cardiomyocyte cell size was measured using ImageJ software and presented as a scatter plot.

Electron microscopy

Samples were also processed for electron microscopy as described previously (Takasato et al., 2015). Sections were analyzed unstained using a Jeol1011 transmission electron microscope (Tokyo, Japan).

Quantitative RT-PCR

Adult human heart RNA from healthy adult humans was obtained from Clontech. RNA was extracted from hCO constructs with Trizol (Thermo Fischer Scientific), according to the manufacturer's instructions and is outlined in the supplementary Materials and Methods. Primer sequences are also outlined in Table S3.

Mitomycin C treatment

hCOs were incubated in 10 µg ml^{-1} mitomycin C in α-MEM 10% FBS with gentle agitation for 90 min in 5% CO_2 at 37°C. hCOs were washed three times in PBS and returned to α-MEM 10% FBS.

Western blotting

Cells were harvested in ice-cold Mammalian Protein Extraction Reagent (Thermo Fisher Scientific) containing complete EDTA-free protease inhibitor and phosphatase inhibitor cocktail tablets (Roche). Protein concentration was determined using a Pierce BCA Protein Assay Kit (Thermo Fisher Scientific) according to the manufacturer's instructions. Protein samples were mixed with Laemmli sample buffer containing 10% β-mercaptoethanol prior to boiling at 95°C for 5 min. Samples were resolved by SDS-PAGE and transferred onto PVDF membrane (Immobilon-P, Merck Millipore). Membranes were blocked with Odyssey blocking buffer (LI-COR Biosciences). Primary antibodies (fibronectin, Abcam, ab2413; or GAPDH, Cell Signaling Technology, 2118S) were prepared in a 1:1 mix of PBS and Odyssey blocking buffer (LI-COR Biosciences) with 1% Tween20. Membranes were treated with the relevant secondary antibody in a 1:1 mix of PBS and Odyssey blocking buffer with 0.1% SDS. Care was taken not to expose secondary antibodies or membranes to light prior to visualization of immunolabeled proteins using an

Development (2017) 144, 1118-1127 doi:10.1242/dev.143966

Odyssey infrared imager (LI-COR Biosciences). Densitometry analysis of membrane was performed using Image Studio Version 5.2 software and fibronectin was normalized to GAPDH.

Force analysis and electrical stimulation of hCO

The active force of hCOs was measured using a Panlab organ bath system at day 14 post-cryoinjury. hCOs were stimulated in Tyrode's solution containing 2 mM calcium under 2 Hz field stimulation, 10 ms rectangular pulses and 200 mV electric current. Labchart Pro was used to record and analyze contractile force. Force was calculated using the average cycle height of contraction and represented as mean active force (mN)±s.e.m.

For calculation of active force from pole movement, a Leica DMi8 inverted high content imager was used to capture a 10 s video of hCOs at 6 h or 14 days post-cryoinjury contracting in real time at 37°C. During recording, hCOs were electrically stimulated in a tissue culture plate at 1 Hz, 10 ms rectangular pulses and ∼100 mV using a conductive wire to transduce electrical current from the organ bath stimulator into the culture medium. Force analysis is detailed in the supplementary Materials and Methods.

Monocyte co-culture

Human cord blood and peripheral blood $CD14^+$ monocytes were co-cultured with HES3 hCOs immediately following cryoinjury in custom well inserts. Subsequently, the hCOs were cultured using our standard protocol. For further details, see supplementary Materials and Methods.

Statistical analysis

Data are represented as mean±s.e.m. and statistical analysis was performed using GraphPad Prism 6. Student's *t*-test and two-way ANOVA were used to determine statistical significance, with $P<0.05$ considered significant.

Acknowledgements

We gratefully acknowledge the help of Charles Ferguson with EM processing and the Australian Microscopy & Microanalysis Research Facility at the Center for Microscopy and Microanalysis, the University of Queensland. We also acknowledge the Developmental Biology Hybridoma Bank for providing the Titin and tropomyosin antibodies, and Shannon O'Brien for assistance with western blotting protocols.

Competing interests

The author(s) declare no competing financial interests. J.E.H is listed as an inventor on patents WO 2015/025030 A1 and WO 2015/040142 Al related to cardiac differentiation and hCO technologies described in this manuscript.

Author contributions

H.K.V., E.R.P. and J.E.H. conceived the experiments. J.E.H., R.J.M. and R.G.P. conducted experiments and analyzed data. D.A.E. provided cell lines. H.K.V. conducted experiments, analyzed data and wrote the manuscript. H.K.V., E.R.P. and J.E.H. analyzed the results. J.E.H. and E.R.P. obtained funding to support the experiments. All authors reviewed and edited the manuscript.

Funding

E.R.P. and J.E.H. are supported by grants and fellowships from the National Health and Medical Research Council of Australia, the National Heart Foundation of Australia, Stem Cells Australia and The University of Queensland. R.G.P. is supported by the National Health and Medical Research Council of Australia (program grant APP1037320 and Senior Principal Research Fellowship 569452) and by the Australian Research Council Centre of Excellence (CE140100036).

Supplementary information

Supplementary information available online at
http://dev.biologists.org/lookup/doi/10.1242/dev.143966.supplemental

References

Aurora, A. B., Porrello, E. R., Tan, W., Mahmoud, A. I., Hill, J. A., Bassel-Duby, R., Sadek, H. A. and Olson, E. N. (2014). Macrophages are required for neonatal heart regeneration. *J. Clin. Invest.* **124**, 1382-1392.

Bergmann, O., Bhardwaj, R. D., Bernard, S., Zdunek, S., Barnabé-Heider, F., Walsh, S., Zupicich, J., Alkass, K., Buchholz, B. A., Druid, H. et al. (2009). Evidence for cardiomyocyte renewal in humans. *Science* **324**, 98-102.

Boulton, J., Henry, R., Roddick, L. G., Rogers, D., Thompson, L. and Warner, G. (1991). Survival after neonatal myocardial infarction. *Pediatrics* **88**, 145-150.

Bryant, D. M., O'meara, C. C., Ho, N. N., Gannon, J., Cai, L. and Lee, R. T. (2014). A systematic analysis of neonatal mouse heart regeneration after apical resection. *J. Mol. Cell. Cardiol.* **79**, 315-318.

Caspi, O., Lesman, A., Basevitch, Y., Gepstein, A., Arbel, G., Habib, I. H. M., Gepstein, L. and Levenberg, S. (2007). Tissue engineering of vascularized cardiac muscle from human embryonic stem cells. *Circ. Res.* **100**, 263-272.

Chablais, F. and Jazwinska, A. (2012). Induction of myocardial infarction in adult zebrafish using cryoinjury. *J. Vis. Exp.* **62**, 1-2.

Chablais, F., Veit, J., Rainer, G. and Jaźwińska, A. (2011). The zebrafish heart regenerates after cryoinjury-induced myocardial infarction. *BMC Dev. Biol.* **11**, 21.

Chen, N., Zhang, J., Xu, M., Wang, Y. L. and Pei, Y. H. (2013). Inhibitory effect of mitomycin C on proliferation of primary cultured fibroblasts from human airway granulation tissues. *Respiration* **85**, 500-504.

Ciulla, M. M., Paliotti, R., Ferrero, S., Braidotti, P., Esposito, A., Gianelli, U., Busca, G., Cioffi, U., Bulfamante, G. and Magrini, F. (2004). Left ventricular remodeling after experimental myocardial cryoinjury in rats. *J. Surg. Res.* **116**, 91-97.

Darehzereshki, A., Rubin, N., Gamba, L., Kim, J., Fraser, J., Huang, Y., Billings, J., Mohammadzadeh, R., Wood, J., Warburton, D. et al. (2015). Differential regenerative capacity of neonatal mouse hearts after cryoinjury. *Dev. Biol.* **399**, 91-99.

Eder, A., Vollert, I., Hansen, A. and Eschenhagen, T. (2016). Human engineered heart tissue as a model system for drug testing. *Adv. Drug Delivery. Rev.* **96**, 214-224.

Elliott, D. A., Braam, S. R., Koutsis, K., Ng, E. S., Jenny, R., Lagerqvist, E. L., Biben, C., Hatzistavrou, T., Hirst, C. E., Yu, Q. C. et al. (2011). NKX2-5(eGFP/w) hESCs for isolation of human cardiac progenitors and cardiomyocytes. *Nat. Methods* **8**, 1037-1040.

Eschenhagen, T., Eder, A., Vollert, I. and Hansen, A. (2012). Physiological aspects of cardiac tissue engineering. *Am. J. Physiol. Heart Circ. Physiol.* **303**, H133-H143.

Evans, M. A., Smart, N., Dube, K. N., Bollini, S., Clark, J. E., Evans, H. G., Taams, L. S., Richardson, R., Levesque, M., Martin, P. et al. (2013). Thymosin beta4-sulfoxide attenuates inflammatory cell infiltration and promotes cardiac wound healing. *Nat. Commun.* **4**, 2081.

Fink, C., Ergün, S., Kralisch, D., Remmers, U., Weil, J. and Eschenhagen, T. (2000). Chronic stretch of engineered heart tissue induces hypertrophy and functional improvement. *FASEB J.* **14**, 669-679.

Frantz, S. and Nahrendorf, M. (2014). Cardiac macrophages and their role in ischaemic heart disease. *Cardiovasc. Res.* **102**, 240-248.

Gonzalez-Rosa, J. M., Martin, V., Peralta, M., Torres, M. and Mercader, N. (2011). Extensive scar formation and regression during heart regeneration after cryoinjury in zebrafish. *Development* **138**, 1663-1674.

Haubner, B. J., Adamowicz-Brice, M., Khadayate, S., Tiefenthaler, V., Metzler, B., Aitman, T. and Penninger, J. M. (2012). Complete cardiac regeneration in a mouse model of myocardial infarction. *Aging* **4**, 966-977.

Haubner, B. J., Schneider, J., Schweigmann, U., Schuetz, T., Dichtl, W., Velik-Salchner, C., Stein, J.-I. and Penninger, J. M. (2016). Functional recovery of a human neonatal heart after severe myocardial infarction. *Circ. Res.* **118**, 216-221.

Hudson, J. E. and Zimmermann, W.-H. (2011). Tuning Wnt-signaling to enhance cardiomyogenesis in human embryonic and induced pluripotent stem cells. *J. Mol. Cell. Cardiol.* **51**, 277-279.

Hudson, J., Titmarsh, D., Hidalgo, A., Wolvetang, E. and Cooper-White, J. (2012). Primitive cardiac cells from human embryonic stem cells. *Stem Cells Dev.* **21**, 1513-1523.

Ieda, M., Tsuchihashi, T., Ivey, K. N., Ross, R. S., Hong, T.-T., Shaw, R. M. and Srivastava, D. (2009). Cardiac fibroblasts regulate myocardial proliferation through beta1 integrin signaling. *Dev. Cell* **16**, 233-244.

Jesty, S. A., Steffey, M. A., Lee, F. K., Breitbach, M., Hesse, M., Reining, S., Lee, J. C., Doran, R. M., Nikitin, A. Y., Fleischmann, B. K. et al. (2012). c-kit+ precursors support postinfarction myogenesis in the neonatal, but not adult, heart. *Proc. Natl Acad. Sci. USA* **109**, 13380-13385.

Lavine, K. J., Epelman, S., Uchida, K., Weber, K. J., Nichols, C. G., Schilling, J. D., Ornitz, D. M., Randolph, G. J. and Mann, D. L. (2014). Distinct macrophage lineages contribute to disparate patterns of cardiac recovery and remodeling in the neonatal and adult heart. *Proc. Natl. Acad. Sci. USA* **111**, 16029-16034.

Macmahon, H. E. (1937). Hyperplasia and regeneration of the myocardium in infants and in children. *Am. J. Pathol.* **13**, 845-854 5.

Mahmoud, A. I., Porrello, E. R., Kimura, W., Olson, E. N. and Sadek, H. A. (2014). Surgical models for cardiac regeneration in neonatal mice. *Nat. Protoc.* **9**, 305-311.

Mercer, S. E., Odelberg, S. J. and Simon, H.-G. (2013). A dynamic spatiotemporal extracellular matrix facilitates epicardial-mediated vertebrate heart regeneration. *Dev. Biol.* **382**, 457-469.

Nahrendorf, M., Swirski, F. K., Aikawa, E., Stangenberg, L., Wurdinger, T., Figueiredo, J.-L., Libby, P., Weissleder, R. and Pittet, M. J. (2007). The healing

myocardium sequentially mobilizes two monocyte subsets with divergent and complementary functions. *J. Exp. Med.* **204**, 3037-3047.
Nieto, A., Cabrera, C. M., Catalina, P., Cobo, F., Barnie, A., Cortes, J. L., Barroso Del Jesus, A., Montes, R. and Concha, A. (2007). Effect of mitomycin-C on human foreskin fibroblasts used as feeders in human embryonic stem cells: immunocytochemistry MIB1 score and DNA ploidy and apoptosis evaluated by flow cytometry. *Cell Biol. Int.* **31**, 269-278.
Opitz, C. A., Leake, M. C., Makarenko, I., Benes, V. and Linke, W. A. (2004). Developmentally regulated switching of titin size alters myofibrillar stiffness in the perinatal heart. *Circ. Res.* **94**, 967-975.
Pinto, A. R., Ilinykh, A., Ivey, M. J., Kuwabara, J. T., D'antoni, M. L., Debuque, R., Chandran, A., Wang, L., Arora, K., Rosenthal, N. A. et al. (2016). Revisiting cardiac cellular composition. *Circ. Res.* **118**, 400-409.
Polizzotti, B. D., Ganapathy, B., Walsh, S., Choudhury, S., Ammanamanchi, N., Bennett, D. G., Dos Remedios, C. G., Haubner, B. J., Penninger, J. M. and Kühn, B. (2015). Neuregulin stimulation of cardiomyocyte regeneration in mice and human myocardium reveals a therapeutic window. *Sci. Trans. Med.* **7**, 281ra45-281ra45.
Porrello, E. R. and Olson, E. N. (2014). A neonatal blueprint for cardiac regeneration. *Stem. Cell Res.* **13**, 556-570.
Porrello, E. R., Mahmoud, A. I., Simpson, E., Hill, J. A., Richardson, J. A., Olson, E. N. and Sadek, H. A. (2011). Transient regenerative potential of the neonatal mouse heart. *Science* **331**, 1078-1080.
Porrello, E. R., Mahmoud, A. I., Simpson, E., Johnson, B. A., Grinsfelder, D., Canseco, D., Mammen, P. P., Rothermel, B. A., Olson, E. N. and Sadek, H. A. (2013). Regulation of neonatal and adult mammalian heart regeneration by the miR-15 family. *Proc. Natl. Acad. Sci. USA* **110**, 187-192.
Poss, K. D., Wilson, L. G. and Keating, M. T. (2002). Heart regeneration in zebrafish. *Science* **298**, 2188-2190.
Robey, T. E. and Murry, C. E. (2008). Absence of regeneration in the MRL/MpJ mouse heart following infarction or cryoinjury. *Cardiovasc. Pathol.* **17**, 6-13.
Sallin, P., de Preux Charles, A. S., Duruz, V., Pfefferli, C. and Jaźwińska, A. (2015). A dual epimorphic and compensatory mode of heart regeneration in zebrafish. *Dev. Biol.* **399**, 27-40.
Schaaf, S., Shibamiya, A., Mewe, M., Eder, A., Stöhr, A., Hirt, M. N., Rau, T., Zimmermann, W.-H., Conradi, L., Eschenhagen, T. et al. (2011). Human engineered heart tissue as a versatile tool in basic research and preclinical toxicology. *PLoS ONE* **6**, e26397.
Skillen, A. W. (1984). Clinical biochemistry of lactate dehydrogenase. *Cell Biochem. Funct.* **2**, 140-144.
Soong, P. L., Tiburcy, M. and Zimmermann, W. H. (2012). Cardiac differentiation of human embryonic stem cells and their assembly into engineered heart muscle. *Curr. Protoc. Cell Biol.* **55**, 3-6.
Sun, Y., Zhang, J. Q., Zhang, J. and Lamparter, S. (2000). Cardiac remodeling by fibrous tissue after infarction in rats. *J. Lab. Clin. Med.* **135**, 316-323.
Synnergren, J., Améen, C., Jansson, A. and Sartipy, P. (2012). Global transcriptional profiling reveals similarities and differences between human stem cell-derived cardiomyocyte clusters and heart tissue. *Physiol. Genomics* **44**, 245-258.
Takasato, M., Er, P. X., Chiu, H. S., Maier, B., Baillie, G. J., Ferguson, C., Parton, R. G., Wolvetang, E. J., Roost, M. S., Chuva de Sousa Lopes, S. M. et al. (2015). Kidney organoids from human iPS cells contain multiple lineages and model human nephrogenesis. *Nature* **526**, 564-568.
Thygesen, K., Alpert, J. S., Jaffe, A. S., Simoons, M. L., Chaitman, B. R., White, H. D., Thygesen, K., Alpert, J. S., White, H. D., Jaffe, A. S. et al. (2012). Third universal definition of myocardial infarction. *Eur. Heart J.* **33**, 2551-2567.
Tiburcy, M., Didie, M., Boy, O., Christalla, P., Doker, S., Naito, H., Karikkineth, B. C., El-Armouche, A., Grimm, M., Nose, M. et al. (2011). Terminal differentiation, advanced organotypic maturation, and modeling of hypertrophic growth in engineered heart tissue. *Circ. Res.* **109**, 1105-1114.
Tiburcy, M., Meyer, T., Soong, P. L. and Zimmermann, W. H. (2014). Collagen-based engineered heart muscle. *Methods Mol. Biol.* **1181**, 167-176.
Tulloch, N. L., Muskheli, V., Razumova, M. V., Korte, F. S., Regnier, M., Hauch, K. D., Pabon, L., Reinecke, H. and Murry, C. E. (2011). Growth of engineered human myocardium with mechanical loading and vascular coculture. *Circ. Res.* **109**, 47-59.
Veerman, C., Kosmidis, G., Mummery, C., Casini, S., Verkerk, A. and Bellin, M. (2015). Immaturity of human stem-cell derived cardiomyocytes in culture: fatal flaw or soluble problem? *Stem Cells Dev.*
Warthin, A. S. (1924). The myocardial lesions of diphtheria. *J. Infect. Dis.* **35**, 32-66.
Yang, Y., Sun, J., Gervai, P., Gruwel, M. L., Jilkina, O., Gussakovsky, E., Yang, X. and Kupriyanov, V. (2010). Characterization of cryoinjury-induced infarction with manganese-and gadolinium-enhanced MRI and optical spectroscopy in pig hearts. *Magn. Reson. Imaging* **28**, 753-766.
Yang, Y., De Gervai, P. D., Sun, J., Gruwel, M. L. and Kupriyanov, V. (2011). Dynamic manganese-enhanced magnetic resonance imaging can detect chronic cryoinjury-induced infarction in pig hearts in vivo. *Contrast Media Mol. Imaging* **6**, 426-436.
Yang, X., Pabon, L. and Murry, C. E. (2014). Engineering adolescence: maturation of human pluripotent stem cell-derived cardiomyocytes. *Circ. Res.* **114**, 511-523.
Zhang, D., Shadrin, I. Y., Lam, J., Xian, H.-Q., Snodgrass, H. R. and Bursac, N. (2013). Tissue-engineered cardiac patch for advanced functional maturation of human ESC-derived cardiomyocytes. *Biomaterials* **34**, 5813-5820.
Zhou, P. and Pu, W. T. (2016). Recounting cardiac cellular composition. *Circ. Res.* **118**, 368-370.
Zimmermann, W.-H., Schneiderbanger, K., Schubert, P., Didié, M., Munzel, F., Heubach, J. F., Kostin, S., Neuhuber, W. L. and Eschenhagen, T. (2002). Tissue engineering of a differentiated cardiac muscle construct. *Circ. Res.* **90**, 223-230.